A Cauchy distribution-based ternary hypothesis testing for bipolar additive watermark detection in H.264/AVC video

L N Chen, G B Yang* and **N B Zhu**
College of Computer and Communication, Hunan University, Changsha 410082, China

Abstract: The statistical distribution of discrete cosine transform (DCT) coefficients is important for video watermarking since they are the main carriers for watermark embedding. For the statistical distribution of intra-coded DCT coefficients in the H.264/AVC video stream, non-parametric hypothesis test is utilised to verify that Cauchy distribution is better than generalised Gaussian distribution (GGD). Moreover, ternary hypothesis test is introduced into the detection of bipolar additive watermarks. By adjusting the watermark strength parameter, the detector performance can be guaranteed. Experimental results show that for those bipolar additive watermarks in the H.264/AVC stream, the proposed approach can achieve a detection accuracy of more than 80% on average.

Keywords: H.264/AVC, digital watermarking, Cauchy distribution, ternary hypothesis testing

1 INTRODUCTION

In the past decade, digital watermarking has attracted a great deal of interest for the copyright protection of digital media. Compared with image watermarking, digital video watermarking differs greatly because of some other strict requirements.[1] First, the watermark embedding, detection and/or extraction should be simple, and try to achieve real-time performance. Second, the watermarked video should be compatible with video coding standard. Third, the watermark detection should be blind. The latest video standard H.264/AVC adopts several new coding features such as variable block size motion estimation/compensation, multiple prediction modes for intra-frame coding and context-adaptive entropy coding. This leads to higher compression efficiency and new challenges for data hiding because of less redundancy existed in H.264/AVC video. Up to now, some video watermarking methods have been proposed for H.264/AVC. Most of them embedded the watermarks into the DCT coefficients[2] or motion vectors,[3] while the rest make full use of new coding features such as context adaptive entropy coding[4] and intra-/inter-prediction modes.[5]

Besides watermark embedding, its detection is also an integral component of a complete watermarking system. Most watermark detection/extraction schemes are designed for specific embedding algorithms. In image watermarking, some general assumptions are made about the statistical distribution of image coefficients to achieve generic detection or extraction.[6] The most representative works are as follows: Huang *et al.* proposed a new detection structure for additive watermark in transform domains based on Huber's robust hypothesis testing theory.[7] A contaminated generalised Gaussian distribution (GGD) is used to model the statistical behaviours of image sub-band coefficients, instead of the perfect GGD. For the optimum detection of transform-domain multiplicative watermarks, a class of generalised correlators is constructed based on the GGD.[8] The square-root detector is designed, which has near optimal performance as a universally

The MS was accepted for publication on 21 November 2010.
* *Corresponding author: Gaobo Yang, College of Computer and Communication, Hunan University, Lushan Road, Changsha 410082, China; email: gbyang_hunu@hotmail.com*

optimal detector for images. Roland *et al.* proposed a lightweight, asymptotically optimal blind detector for additive spread-spectrum watermark.[9] The marginal distributions of discrete wavelet transform detail sub-band coefficients are modelled by one-parameter Cauchy distributions, and a Rao hypothesis test is derived to detect watermarks of unknown amplitude in Cauchy noise. Compared with image watermarking, few works have been carried out on the generic detection/extraction in video watermarking. Since discrete cosine transform (DCT) coefficients are the main carriers for video watermarking algorithms, it will also be possible to achieve generic detection by modelling their statistical distribution, at least for some specific type of video watermarking. For the latest H.264/AVC video standard, its intra-coded DCT coefficients are modelled with Gaussian, Laplacian or Cauchy distribution. These statistical distributions have been utilised for various purposes such as rate control[10] and object detection.[11] Furthermore, GGD is verified to be better than Laplacian distribution in portraying the distribution of its AC coefficients. A theoretical framework for watermark detection is also developed based on a likelihood ratio test.[12] However, it is of high computational complexity and cannot realise watermark extraction. It is worthy of further investigation for the watermark detection/extraction in the H.264/AVC video by making full use of the statistical distribution of its DCT coefficients.

Motivated by the introduction of Gaussian distribution into watermark detection, we proposed a robust detection scheme of bipolar additive watermarks in the H.264/AVC video. The contributions of this paper are the non-parametric hypothesis test for the comparison between Cauchy distribution and GGD when modelling the intra-coded DCT coefficients, and further investigation of blind detection of bipolar additive watermark by ternary hypothesis test. The rest paper is organised as follows. In Section 2, Cauchy distribution and GGD are utilised to model the statistical distribution of intra-coded DCT coefficients for H.264/AVC and their parameters are estimated by maximum-likelihood estimation (MLE), respectively. In Section 3, Cauchy distribution is introduced into watermark detection by ternary hypothesis testing. Section 4 discusses the influence of watermark strength to its detection accuracy. Experimental results are presented in Section 5 and we conclude this paper in Section 6.

2 NON-PARAMETRIC HYPOTHESIS TEST OF THE DCT COEFFICIENT DISTRIBUTION

For those intra-coded DCT coefficients in the H.264/AVC video, it is verified by experiments that GGD is superior to Laplacian distribution because it describe their distribution more accurately. Gaussian distribution and GGD model are most widely used to model the statistical distribution of DCT coefficients in H.264/AVC. Though it is claimed in Refs. 10 and 11 that Cauchy distribution is more accurate than Laplacian distribution in most cases, no goodness-of-fit tests are performed to verify this. In statistics, MLE is a method of estimating the parameters of a statistical model. In this section, MLE is utilised to estimate those parameters of GGD and Cauchy distribution, and the Kolmogorov–Smirnov (K–S) and χ^2 tests are used to determine the better-fit distribution.

2.1 The GGD and Cauchy distribution models

The GGD is a parametric family of symmetric distributions. For a random variable in the form of GGD with mean μ, scale parameter β and shape parameter α, its probability density function (PDF) is given by

$$f(x,\alpha,\beta,\mu)=\left[\frac{\alpha}{2\beta\Gamma(1/\alpha)}\right]\exp\left(-\left|\frac{x-\mu}{\beta}\right|^{\alpha}\right),\quad x\in R \quad (1)$$

where

$$\beta=\left[\frac{\sigma^2\Gamma(1/\alpha)}{\Gamma(3/\alpha)}\right]^{1/2}=\sigma\left[\frac{\Gamma(1/\alpha)}{\Gamma(3/\alpha)}\right]^{1/2},\qquad \Gamma(z)=\int_0^{\infty}e^{-t}t^{z-1}\mathrm{d}t \quad (2)$$

and σ is standard deviation.

In contrast to the Gaussian distribution (which arises as a special case of the GGD for $\alpha=2$), the GGD is a leptokurtic distribution which allows heavy-tails. For the statistics of those DCT coefficients, α and σ should be estimated. Their final results by MLE[13] are as follows

$$\frac{\psi(1/\alpha+1)+\log(\alpha)}{\alpha^2}+\frac{1}{\alpha^2}\log\left(\frac{1}{n}\sum_{i=1}^{n}|x_i|^{\alpha}\right)-\frac{\sum_{i=1}^{n}|x_i|\alpha\log|x_i|}{\alpha\sum_{i=1}^{n}|x_i|^{\alpha}}=0 \quad (3)$$

$$\widehat{\sigma}=\left[\frac{\widehat{v}\alpha(\widehat{v}\sum_{i=1}^{n}|x_i|^{\widehat{v}})}{n}\right]^{1/\widehat{v}} \quad (4)$$

where

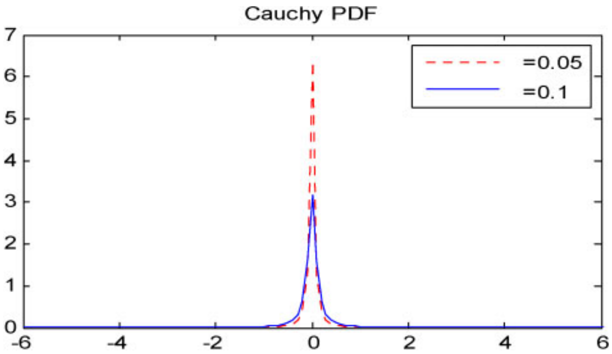

1 The PDF of Cauchy distribution (a=0)

$\Psi(\tau)=-r+\int_0^1(1-t^{\tau-1})(1-t)^{-1}\mathrm{d}t$, and x_i denotes the DCT coefficients, index i denotes the ith DCT coefficient and n is the number of DCT samples.

For Cauchy distribution, its PDF can be written as

$$f(x)=\frac{1}{\pi}\frac{\lambda}{\lambda^2+(x-\alpha)^2} \tag{5}$$

where λ and a are shape and position parameter, respectively ($-\infty<\alpha<\infty$, $\lambda>0$). For a random variable with such a PDF, it is denoted by $X\sim C(\lambda,a)$. Figure 1 is a typical histogram of those alternating current coefficients for an 8×8 block in *Akiyo* sequence. It is symmetric around zero.

For the statistics of DCT coefficients, a will be zero.[14] Thus, only one parameter λ is necessary to be estimated. The final result is derived by MLE[13] as follows

$$\frac{1}{n}\sum_{i=1}^{n}\frac{2}{1+(x_i/\hat{\lambda})^2}-1=0 \tag{6}$$

2.2 Non-parametric hypothesis test

In the following, MLE is used to estimate the parameters of GGD and Cauchy distribution. Goodness-of-fit tests are usually utilised to examine the hypothesis that a given dataset comes from a model distribution with given parameters. The KS test and χ^2 test are two popular goodness-of-fit tests.[15] Therefore, they are chosen to verify whether GGD or Cauchy distribution is better for the DCT coefficients in H.264/AVC. In the experiments, three typical test sequences such as *Akiyo*, *Foreman* and *News* are encoded with the H.264/AVC reference code JM8.6. The encoder parameters are set as follows: frame rate=30 frames s^{-1}, GOP=IIIII, QP=16. For every sequence, those DCT coefficients of the first 10 frames are used for hypothesis tests. There are about 23750 samples for every frame. The significant level is set to be 0.05. Experimental results are analysed with statistical software SPSS and summarised in Table 1. Apparently, Cauchy distribution is superior to GGD when they are used to model the intra-coded DCT coefficients. For most frames, the K–S and χ^2 values of Cauchy distribution are less than those of GGD. However, there are still some errors for several samples. For example, for the sixth frame of *Akiyo* sequence, the K–S value of Cauchy distribution is larger that that of GGD. These few samples different from the total distribution are referred as singular samples in the statistical theory. If only large amounts of samples are experimented and the singular samples are removed from statistics, optimal statistical results can be obtained.

3 WATERMARK DETECTION AND EXTRACTION

In the following, Cauchy distribution is exploited for the detection and extraction of bipolar additive watermark in the H.264/AVC video. We make no assumption that the embedding strength is known to watermark detector. For additive watermark, its embedding rule is given by

$$x[n]=t[n]+\theta w[n],\ n=0,\ 1,\ \ldots,\ N \tag{7}$$

where θ denotes the watermark strength, $x[n]$ is a watermarked DCT coefficient and $t[n]$ is a host image coefficient. Since the original DCT coefficients meet Cauchy distribution with parameter a=0, the watermark detection problem can be formulated as a problem of deterministic signal detection of unknown amplitude (i.e. our watermark) from a Cauchy-distributed noise (i.e. the DCT coefficients) with unknown shape parameter.[6] This is actually a composite hypothesis testing problem. It can be formulated as a three-sided parameter test as follows

$$\begin{aligned}&H_0:\ x[n]=t[n]+\theta,\ \text{without watermark}\\&H_1:\ x[n]=t[n]+\theta,\ \text{with watermark and watermark bit equals}+1\\&H2:\ x[n]=t[n]-\theta,\ \text{with watermark and watermark bit equals}-1\end{aligned} \tag{8}$$

Since $t[n]$ meets Cauchy distribution, $t\sim C(\lambda,0)$, MLE is utilised to estimate λ. The prior probabilities of these three hypotheses are unknown, and the Bayes decision rule is equivalent to MLE.[11] Their PDFs of H_0, H_1 and H_2 are defined as follows

$$p(x|H_0)=\frac{1}{\pi}\frac{\lambda_w}{\lambda_w^2+x^2} \tag{9}$$

$$p(x|H_1)=\frac{1}{\pi}\frac{\lambda_w}{\lambda_w^2+(x+\theta)^2} \tag{10}$$

$$p(x|H_2)=\frac{1}{\pi}\frac{\lambda_w}{\lambda_w^2+(x-\theta)^2} \tag{11}$$

According to the MLE criteria, if every DCT coefficient is computed as equations (9)–(11), the decision that which kind of hypothesis is correct can be made by maximising the equation (12)

$$\max p(x|H_i) \tag{12}$$

During the watermark detection process, if H_1 or H_2 is true and the decision of H_1 or $H_2$is the same, this kind of detection probability is referred to the desired probability of true detection, which is denoted as P_D. If H_0 is true but H_1 or H_2 is decided to be true, this can be referred as the first class of errors. The probability of this kind of false alarm is denoted as P_{FA}. On the contrary, if H_1 or H_2 is true, yet H_0 is decided to be true, it is referred as the second class of errors. The probability of this kind of missed alarms is denoted as P_m. As shown in Fig. 2, both these two kinds of errors are inevitable, but they can be compromised by adjusting the threshold selection.

Let x_1 and x_2 be the thresholds for H_1or H_2, respectively, they should meet $x_1=-x_2=-a$. Apparently, the decrease of the first kind of error probability is at the sacrifice of the increase of the second kind of error probability. It is impossible to decrease these two kinds of error probabilities simultaneously. For the design of an optimal watermark detector, its goal will be to decrease one while maintaining the other. It can be achieved by selecting appropriate threshold to maximise P_D which maintaining a constraint $P_{FA}=\delta$.[14] Following the work in Ref. 12, the definitions of P_{FA}, P_D and P_m can be further derived as follows

$$P_{FA}=\int_a^{+\infty}\frac{1}{\pi}\frac{\lambda_w}{\lambda_w^2+x^2}dx=\frac{1}{2}-\frac{1}{\pi}\arctan\left(\frac{a}{\lambda_w}\right) \tag{13}$$

Table 1 The hypothesis tests of GGD and Cauchy distribution for the DCT coefficients

	GGD				Cauchy distribution		
Video sequence (frame number)	$\hat{v}$	$\hat{\sigma}$	χ^2	K–S	$\hat{\lambda}$	χ^2	K–S
Foreman(1)	0.48	6.31	5868.378	0.9989	0.1084	1760.371	0.9948
Foreman(2)	0.43	6.35	5628.601	0.9989	0.1075	1717.87	0.9929
Foreman(3)	0.53	6.34	5531.655	0.9992	0.1079	1706.992	0.9929
Foreman(4)	0.54	6.16	5565.991	0.9992	0.1089	1887.599	0.9917
Foreman(5)	0.65	5.02	6957.270	0.9992	0.1092	1775.741	0.9928
Foreman(6)	0.76	4.05	5869.378	0.9989	0.1087	1735.561	0.9938
Foreman(7)	0.90	3.37	5954.207	0.9992	0.1100	2022.762	0.9937
Foreman(8)	0.47	3.06	3712.979	0.9992	0.1097	1846.227	0.9931
Foreman(9)	0.42	4.46	3992.861	0.9992	0.1097	1653.25	0.9911
Foreman(10)	0.44	4.59	4102.586	0.9992	0.1107	1969.031	0.9904
Akiyo(1)	0.59	6.31	3768.135	0.9946	0.1043	344.417	0.9835
Akiyo(2)	0.67	6.35	3610.844	0.9946	0.1041	348.265	0.9835
Akiyo(3)	0.78	6.34	3449.321	0.9946	0.1043	329.468	0.9835
Akiyo(4)	0.50	6.16	3943.867	0.9946	0.1049	341.288	0.9834
Akiyo(5)	0.45	5.02	3963.610	0.9946	0.1050	351.103	0.9834
Akiyo(6)	0.46	4.05	3821.268	0.9946	0.1050	387.267	0.9994
Akiyo(7)	0.53	3.37	3930.060	0.9946	0.1047	365.663	0.9835
Akiyo(8)	0.61	3.83	3876.361	0.9946	0.1048	381.509	0.9835
Akiyo(9)	0.68	3.29	3708.592	0.9946	0.1048	362.541	0.9834
Akiyo(10)	0.59	3.45	3656.028	0.9946	0.1050	359.734	0.9834
News(1)	0.75	3.39	6807.505	0.9960	0.1203	3573.171	0.9883
News(2)	0.72	2.94	7393.046	0.9960	0.1207	3547.837	0.9883
News(3)	0.72	2.77	7418.455	0.9960	0.1204	3552.015	0.9883
News(4)	0.68	2.73	7460.378	0.9960	0.1201	3365.257	0.9884
News(5)	0.77	2.66	8004.884	0.9960	0.1196	3399.943	0.9897
News(6)	0.75	2.57	7775.774	0.9960	0.1200	3346.851	0.9896
News(7)	0.76	2.88	7711.350	0.9960	0.1205	3458.819	0.9883
News(8)	0.81	3.15	7760.783	0.9960	0.1202	3460.382	0.9896
News(9)	0.88	2.98	7621.812	0.9960	0.1201	3343.308	0.9896
News(10)	0.87	3.23	7588.809	0.9960	0.1197	3259.964	0.9884

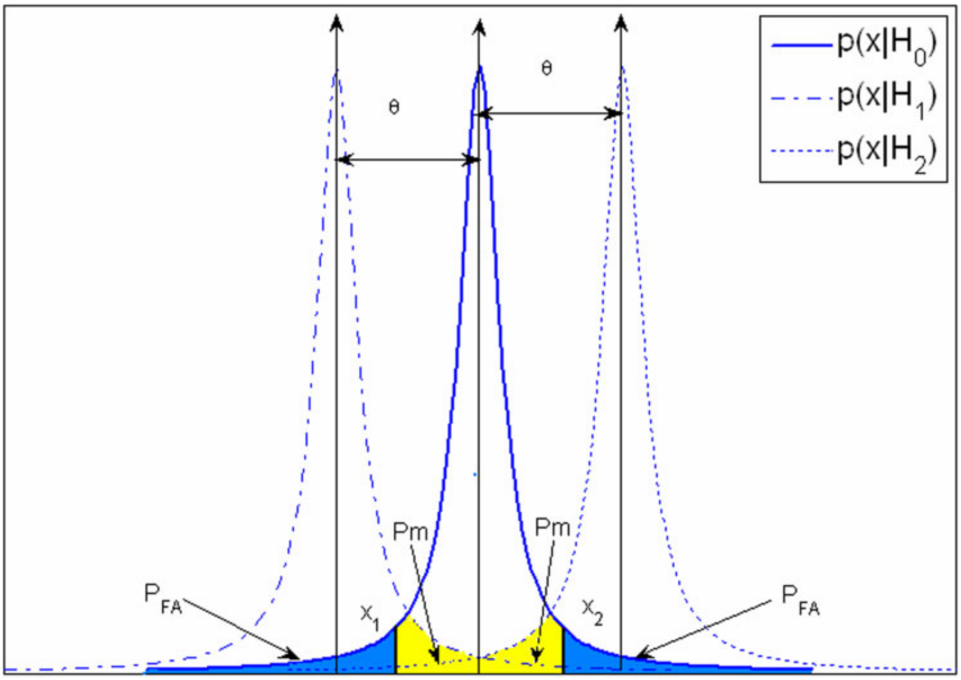

2 The PDFs of H_0, H_1 and H_2

$$P_{\mathrm{D}}=\int_{\mathrm{a}}^{+\infty}\frac{1}{\pi}\frac{\lambda_{\mathrm{w}}}{\lambda_{\mathrm{w}}^2+(x-\theta)^2}\mathrm{d}x$$
$$=\frac{1}{2}-\frac{1}{\pi}\arctan\left(\frac{a-\theta}{\lambda_{\mathrm{w}}}\right) \tag{14}$$

$$P_{\mathrm{m}}\approx\int_{0}^{\mathrm{a}}\frac{1}{\pi}\frac{\lambda_{\mathrm{w}}}{\lambda_{\mathrm{w}}^2+(x-\theta)^2}\mathrm{d}x$$
$$=\frac{1}{\pi}\arctan\left(\frac{a-\theta}{\lambda_{\mathrm{w}}}\right)+\frac{1}{\pi}\arctan\left(\frac{\theta}{\lambda_{\mathrm{w}}}\right) \tag{15}$$

For a given P_{FA}, the thresholds of x_{i} and x_2 are derived from equation (13) as

$$x_1=-\lambda_{\mathrm{w}}\tan\left[\pi\left(\frac{1-2P_{\mathrm{FA}}}{2}\right)\right] \tag{16}$$

$$x_2=\lambda_{\mathrm{w}}\tan\left[\pi\left(\frac{1-2P_{\mathrm{FA}}}{2}\right)\right] \tag{17}$$

For a given $P_{\mathrm{FA}}=\delta$, the largest PDF should be made among the three hypothesis H_0, H_1 and H_2 in terms of equation (12). When the DCT coefficient is less than x_{i}, $p(x|H_1)$ will be the largest. When the DCT coefficient is between the thresholds x_{i} and x_2, $p(x|H_0)$ will be the largest. When the DCT coefficient is less than x_2, $p(x|H_2)$ will be the largest. Thus, watermark detection is converted to a problem of comparing the DCT coefficient with thresholds. Let x_{i} be the DCT coefficient to be detected, if it is less than x_1, the watermark bit will be -1. If x_{i} is between x_1 and x_2, there is no watermark bit. If x_{i} is larger than x_2, the watermark bit will be $+1$.

4 ANALYSIS OF DETECTOR PERFORMANCE WITH THE WATERMARK STRENGTH PARAMETER

In general, watermark detection is closely related to its strength. In this section, the watermark detector performance is analysed for different embedding strengths. When the watermark strength is set to 1 during the embedding process, the detection results with a given false alarm probabilities are summarised in Tables 2 and 3.

From Tables 2 and 3, it can be found that when there is no adjustment of watermark strength ($\theta=1$), P_{FA} and P_{m} are relatively high, yet P_{D} is quite low. To obtain better detection performance, the watermark strength θ should be adjusted. From the watermark embedding point of view, its strength θ is adjusted to minimise the visual distortion and the bit rate increase. We vary θ from 1 to 5 in the experiments. From Fig. 3, it can be found that when $P_{\mathrm{FA}}=10^{-1}$ and $\theta=3$, the detector achieves satisfactory performance because of a quite high P_{D} and low P_{m}. Especially, as shown in Fig. 4, when P_{FA} is further lowered, the response of $P_{\mathrm{D}}-P_{\mathrm{FA}}$ increases quite rapidly and the response of $P_{\mathrm{m}}-P_{\mathrm{FA}}$ decreases quite acutely, and the desired P_{D} and P_{m} can be obtained.

In general, the watermark strength should be low in order to keep the transparency of embedded watermark. However, the desired watermark detection performances here are obtained by increasing the watermark strength, which seems to be contradictory with the general requirements of video watermarking. Nevertheless, the proposed watermark detection scheme is still useful. The reasons are summarised as follows: First, for some video watermarking algorithms, since the watermark capacity is quite high, its transparency can still be guaranteed by making compromise between capacity and strength. Second, the increase in watermark strength does benefit to the purpose of copyright protection for digital video because it will be more difficult to be removed. For example, the watermarking algorithm in Ref. 2 can be designed as follows since it is of high watermark capacity.

$\theta=3$, when $P_{FA}=10^{-1}$

$\theta=5$, when $P_{FA}=10^{-2}$–10^{-1}

5 EXPERIMENTAL RESULTS AND DISCUSSION

5.1 Watermark embedding

Four typical video sequences in QCIF format are selected for experiment. They are encoded with JM8.6 reference code (frame rate=30, GOP=IPPPP, QP=16). The watermark embedding algorithms in[12,16,17] are used for detection, respectively. In Ref. 12, it employs Watson visual model for 4×4 DCT block to obtain a larger payload and a greater robustness while minimising visual distortion. Due to space restriction, only the watermark embedding results for Ref. 12 are summarised in Table 4. Its watermark strength θ is set as 3 and 5, respectively. On average, the peak signal-to-noise ratio (PSNR) decrease is less that 5% and bit rate increase is about 8%. Therefore, satisfactory performance of watermark embedding is still guaranteed, even though the watermark strength is relative high. Moreover, the watermark capacity is still acceptable.

5.2 The detection of bipolar additive watermark

The watermark detection and extraction are performed at the decoder. For a specified P_{FA}, the thresholds for x_1 and x_2 will be a and $-a$, respectively. By making comparison between the decoded DCT coefficients and these thresholds, the watermark bit can be obtained. The experimental results of watermark detection and extraction are summarised in Table 5. If P_{FA} equals 10^{-2}, it can detect relatively more watermark bits. However, due to the relatively low thresholds, some of DCT coefficients without watermark will be regarded as with watermark. If P_{FA} is decreased to 10^{-3}, the correctly detected watermark bits will be less than that when P_{FA} equals 10^{-2}. This is because with the

Table 2 The detection results when $P_{FA}=0.01$–0.02 and $\theta=1$

Foreman, $\lambda_w=0.1201$					*Akiyo*, $\lambda_w=0.1120$				
P_{FA}	P_D	P_M	x_1	x_2	P_{FA}	P_D	P_M	x_1	x_2
0.010	0.0135	0.9484	−3.8185	3.8185	0.010	0.0139	0.9506	−3.5639	3.5639
0.011	0.0154	0.9465	−3.4711	3.4711	0.011	0.0159	0.9486	−3.2397	3.2397
0.012	0.0175	0.9423	−3.1816	3.1816	0.012	0.0181	0.9464	−2.9695	2.9695
0.013	0.0197	0.9399	−2.9366	2.9366	0.013	0.0205	0.9440	−2.7408	2.7408
0.014	0.0221	0.9373	−2.7266	2.7266	0.014	0.0230	0.9415	−2.5448	2.5448
0.015	0.0247	0.9345	−2.5446	2.5446	0.015	0.0259	0.9386	−2.3750	2.3750
0.016	0.0275	0.9314	−2.3853	2.3853	0.016	0.0290	0.9355	−2.2263	2.2263

Table 3 The detection results when $P_{FA}=10^{-3}$–10^{-2} and $\theta=1$

Foreman, $\lambda_w=0.1201$					*Akiyo*, $\lambda_w=0.1120$				
P_{FA}	P_D	P_M	x_1	x_2	P_{FA}	P_D	P_M	x_1	x_2
0.001	0.001	0.9610	−38.1971	−38.1971	0.001	0.0010	0.9635	−35.6506	35.6506
0.002	0.0021	0.9599	−19.0983	−19.0983	0.002	0.0021	0.9624	−17.8251	17.8251
0.003	0.0033	0.9587	−12.7320	−12.7320	0.003	0.0033	0.9612	−11.8832	11.8832
0.004	0.0045	0.9575	−9.5488	−9.5488	0.004	0.0045	0.9600	−8.9122	8.9122
0.005	0.0058	0.9562	−7.6388	−7.6388	0.005	0.0058	0.9587	−7.1296	7.1296
0.006	0.0071	0.9549	−6.3654	−6.3654	0.006	0.0072	0.9573	−5.9411	5.9411
0.007	0.0086	0.9534	−5.4559	−5.4559	0.007	0.0087	0.9558	−5.0921	5.0921

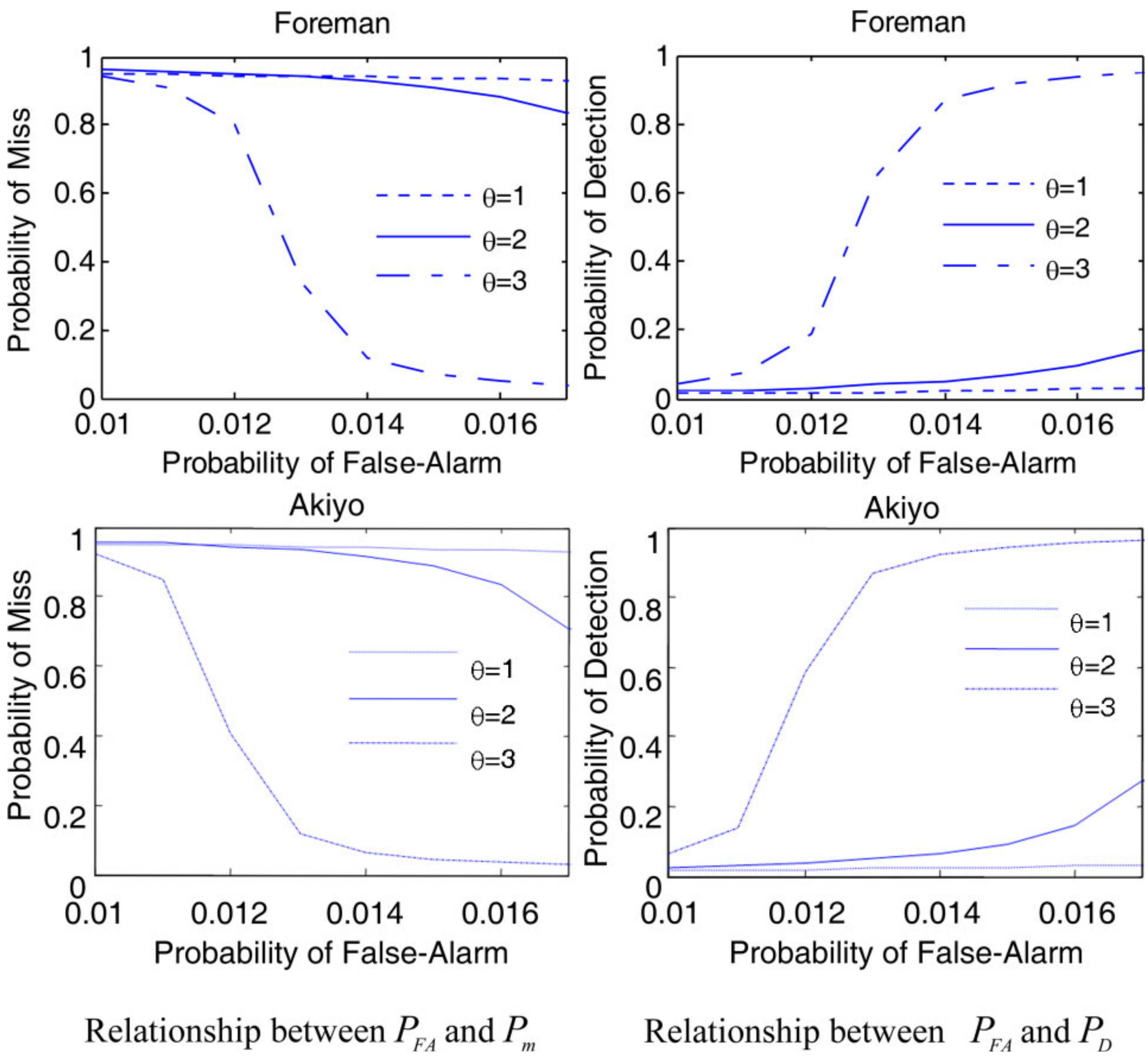

3 The relationship between P_{FA}, P_{D} and P_{m} ($P_{\mathrm{FA}}=10^{-1}$)

decrease of specified P_{FA}, the possibility of P_{M} will be increased as what discussed in Section 3. However, due to a relatively low P_{FA}, the precision of correct detection still can be kept more than 83%.

This kind of ternary hypothesis testing-based watermark detection is effective. Theoretically, no matter what kinds of video watermarking algorithm, if it is embedded with bipolar additive watermark with mean 0 and variance 1 and the watermark strength is reasonably adjusted, the proposed approach can realise satisfactory watermark detection. It should be mentioned that the utilisation of Cauchy distribution to model the DCT coefficients is in fact a statistical analysis, and there will be some detection errors for those singular samples. However, the ratio of correct detection can maintain at least 80%.

To further demonstrate the detector performance, non-geometric attacks such as compression with different bit rates or adding noise are performed on the watermarked bit-stream. The watermarked video by Ref. 12 is re-compressed with a fixed compression ratio, and the proposed detector is used to detect the possible watermark bits from the re-compressed video. The experimental results are summarised in Table 6. Apparently, under recompression with a fixed compression ratio 50, both the detected watermark bits and the correctly detected watermark bits are very near to those in Table 5. The detector performance is robust to re-compression attacks

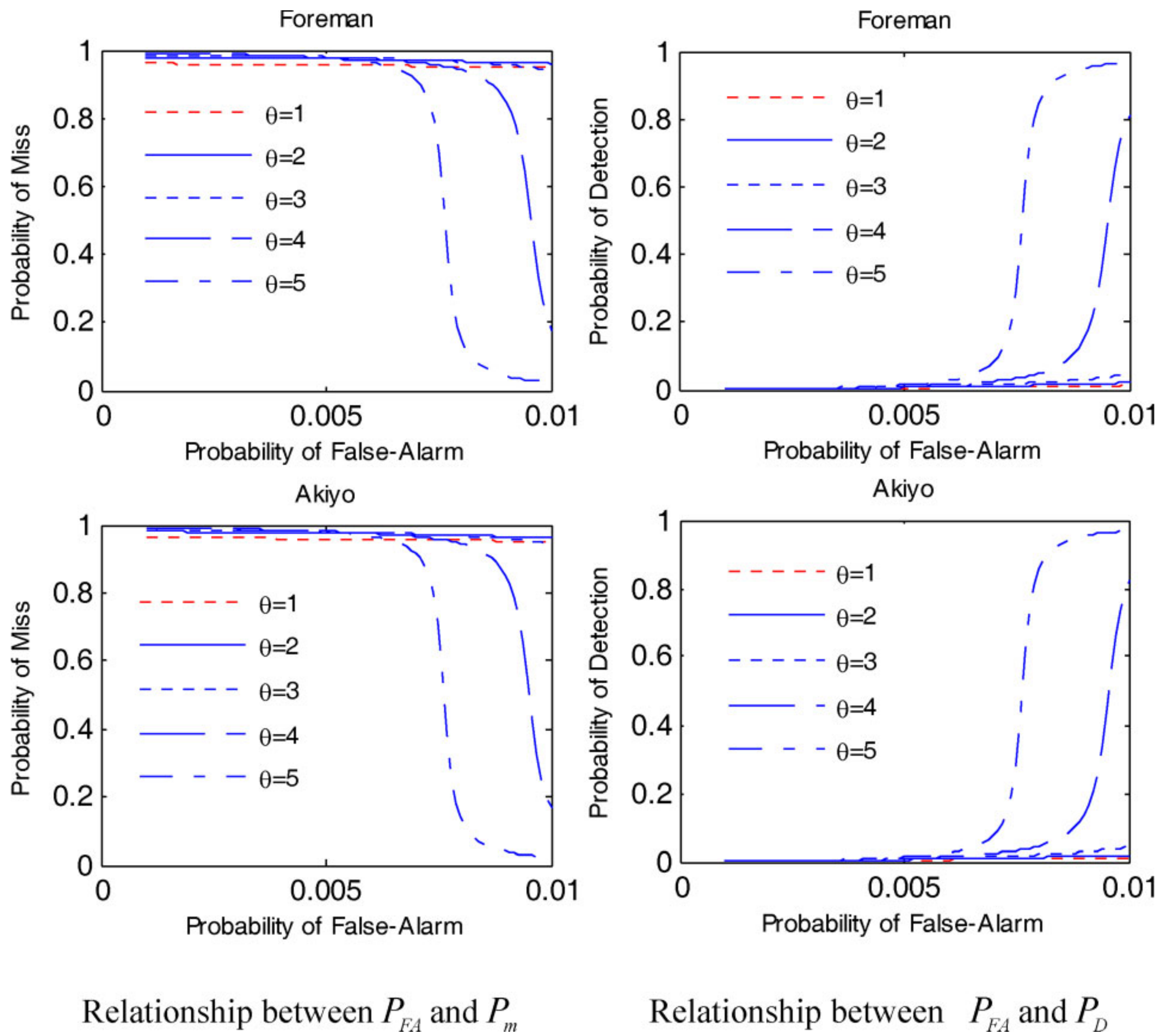

4 The relationship between P_{FA}, P_{D} and P_{m} ($P_{\mathrm{FA}}=10^{-2}$–10^{-1})

simply because the proposed detector is a statistical analysis based approach. The re-compression will not change the Cauchy distribution of those intra-coded DCT coefficients in H.264/AVC, and thus, the ternary hypothesis test is still valid for those watermarked bits. However, when additive white noise is added into the watermarked bitstream, the detector's performance degrades significantly. For these four video sequences, their detection probabilities P_{D} are only about 32% on average. The reasons are twofold. First, the added extra noise has bad effects on the distribution of DCT coefficients. Second, the white noise might mix with the watermark bit, which brings extra difficulty for watermark detection.

Table 4 Performance of watermark embedding

Video sequences	θ	Watermark capacity	PSNR decrease	Bit rate increase
News	3	265	2.48%	8.36%
	5	265	3.15%	10.27%
Foreman	3	160	1.92%	3.69%
	5	160	2.30%	6.14%
Akiyo	3	124	1.55%	7.50%
	5	124	2.22%	9.86%
Mother	3	86	1.03%	5.52%
	5	86	1.58%	8.24%

5.3 analysis of threshold α

In the proposed approach, an important threshold for watermark detection is a. Its definition is as follows

Table 5 Experimental results for watermark detection

Video sequence	θ	P_D	P_{FA}	a	Watermark capacity per frame (bit)	The detected watermark (bit)	Correctly detected watermark (bit)	Ratio of correct detection Ref. 12	Ref. 16	Ref. 17
News	3	93.81%	1.6%	2.3893	265	247	243	86.73%	75.21%	82.23%
	5	93.18%	0.86%	4.4479	265	206	202	89.58%	82.39%	84.77%
Foreman	3	96.17%	1.9%	2.0008	160	161	153	91.36%	69.13%	87.67%
	5	93.28%	0.86%	4.4405	160	147	142	89.31%	73.65%	89.91%
Akiyo	3	96.08%	1.7%	2.0951	124	122	116	84.77%	83.92%	82,54%
	5	93.08%	0.85%	4.1932	124	109	105	86.44%	86.44%	84.67%
Mother	3	97.01%	1.86%	3.0125	86	91	75	83.46%	72.47%	74.65%
	5	92.56%	0.75%	5.1364	86	82	73	86.73%	78.85%	76.82%

Table 6 The detector performance under re-compression attack

Video sequence	θ	Compression ratio	Watermark capacity per frame (bit)	The detected watermark (bit)	The Correctly detected watermark (bit)
News	3	50	265	242	236
	5	50	265	205	201
Foreman	3	50	160	158	147
	5	50	160	145	138
Mother	3	50	86	90	72
	5	50	86	80	70

$$\alpha = \lambda_w \tan\left[\pi\left(\frac{1-2P_{FA}}{2}\right)\right] \tag{18}$$

where P_{FA} is the desired false alarm probability and λ_w is obtained by MLE. It can be found from equation (6) that the computation of λ_w depends on the original video stream. From the experimental results in Table 5, it is found that the threshold α varies between 2 and 7 for most video sequences. If we set a limit for α and make it vary between the maximum and minimum values, the watermark detection can be realised without the computation of λ_w from the original video stream.

6 CONCLUSIONS

Based on the theory of non-parametric hypothesis test, it is verified that Cauchy distribution is better than GGD when they are used to model the statistical distribution of those intra-coded DCT coefficients by H.264/AVC. Furthermore, ternary hypothesis test is introduced into the detection of bipolar additive watermark. The experimental results show that for those bipolar additive watermarks in H.264/AVC stream, the proposed approach can achieve a detection accuracy of more than 80% on average. However, the limitation for the proposed approach is the strong relation between detector performance and watermark strength. Moreover, the extension of the proposed detection approach to other DCT coefficients-based video watermarking algorithm is worthy of further investigation.

ACKNOWLEDGEMENTS

This work is supported in part by the Special Prophase Project on National Basic Research Program of China (2010CB334706), National Natural Science Foundation of China (61072122), Key Project of Hunan Provincial Natural Science Foundation (11JJ2053) and the Fundamental Research Funds for the Central Universities (Hunan University).

REFERENCES

1 Zhang, J., Ho, A. T. S., Qiu, G. and Marziliano, P. Robust video watermarking of H.264/AVC. *IEEE Tran. Circuits Syst.-II: Express Briefs*, 2007, **54**, 205–209.
2 Wu, C., Zheng, Y., Ip, W. H., Chan, C. Y., Yung, K. L. and Lu, Z. M. A flexible H.264/AVC compressed video watermarking scheme using particle swarm optimization based dither modulation. *Int. J. Electron. Commun.*, 2011, **65**, 27–36.
3 Ma, X., Li, Z., Tu, H. and Zhang, B. A data hiding algorithm for H.264/AVC video streams without intra-frame distortion drift. *IEEE Trans. Circuits Syst. Video Technol.*, 2010, **20**, 1320–1330.

4 Mansouri, A., Aznaveh, A. M., Azar, F. T. and Kurugollu, F. A low complexity video watermarking in H.264/AVC compressed domain. *IEEE Trans. Inf. Forensics Secur*., 2010, **5**, 649–657.

5 Yang, G., Li, J., He, Y. and Kang, Z. An information hiding algorithm based on intra-prediction modes and matrix coding for H.264/AVC video stream. *Int. J. Electron. Commun*., 2011, **65**, 331–337.

6 Meerwald, P. and Uhl, A. Watermark detection on quantized transform coefficients using product Bernoulli distributions, Proc. ACM Workshop on *Multimedia and security: MM&Sec'10*, Roma, Italy, September 2010, ACM, pp. 175–179.

7 Huang, X. and Zhang, B. Robust detection of additive watermarks in transform domains. *IEE Proc. Inf. Secur*., 2006, **153**, 97–106.

8 Cheng, Q. and Huang, T. S. Robust optimum detection of transform domain multiplicative watermarks. *IEEE Trans. Signal Process*., 2003, **51**, 906–923.

9 Roland, K., Peter, M. and Andreas, U. A lightweight Rao-Cauchy detector for additive watermarking in the DWT-domain, Proc. ACM Workshop on *Multimedia and security: MM&Sec'08*, Oxford, UK, September 2008, ACM, pp. 33–42.

10 Kamaci, N., Altunbasak, Y. and Mersereau, R. M. Russell frame bit allocation for the H.264/AVC video coder via Cauchy-density-based rate and distortion models. *IEEE Trans. Circuits Syst. Video Technol*., 2005, **15**, 994–1006.

11 Zhou, T., Zhuang, M. and Xiong, Z. Generalized Gaussian distribution to early detect zero quantized discrete cosine transform coefficients in H.264/AVC video encoding. *IET Image Process*., 2010, **4**, 473–485.

12 Maneli, N. and Russell, M. A framework for robust watermarking of H.264 encoded video with controllable detection performance. *IEEE Trans. Inf. Forensics Secur*., 2007, **2**, 14–23

13 Levy, B. C. Principles of Signal Detection and Parameter Estimation, 2008 (Springer, New York).

14 Altunbasak, Y. and Kamaci, N. An analysis of the DCT coefficient distribution with the H.264 video coder, Proc. IEEE Int. Conf. on *Acoustics, speech, and signal processing: ICASSP '04*, Montreal, Que., Canada, May 2004, IEEE Signal Processing Society, pp. 77–80.

15 Lilliefors, H. On the Kolmogorov–Smirnov test for normality with mean and variance unknown. *J. Am. Stat. Assoc*., 1967, **62**, 399–402.

16 Kuo, M. H. A novel robust watermarking technique using IntDCT based AC. *WSEAS Trans. Comput*., 2008, **7**, 16–24.

17 Maneli, N. and Russell, M. M. Compressed-domain video watermarking for H.264, Proc. IEEE Int. Conf. on Image Processing: *ICIP 2005*, Genoa, Italy, September 2005, IEEE, Vol. 2, pp. 890–893.